JOC The Journal of Organic Chemistry

pubs.acs.org/joc Featured Article

Divergent Total Syntheses of (−)-Pseudocopsinine and (−)-Minovincinine

Xianhuang Zeng, Vyom Shukla, and Dale L. Boger*

Cite This: https://dx.doi.org/10.1021/acs.joc.0c02493 Read Online

ACCESS | Metrics & More | Article Recommendations | Supporting Information

ABSTRACT: Herein, the first total syntheses of (−)-pseudocopsinine (**1**) and (−)-minovincine (**3**) from a common intermediate **8** are detailed, enlisting late-stage, hydrogen atom transfer (HAT)-mediated free radical bond formations (C20−C2 and C20−OH, respectively) that are unique to their core or structure. The approach to **1** features an Fe-mediated HAT reaction of the intermediate olefin **2**, effecting a transannular C20−C2 free radical cyclization of a challenging substrate with formation of a strained [2.2.1] ring system and reaction of a poor acceptor tetrasubstituted alkene with a hindered secondary free radical to form a bond and quaternary center adjacent to another quaternary center. Central to the assemblage of their underlying *Aspidosperma* skeleton is a powerful [4 + 2]/[3 + 2] cycloaddition cascade of 1,3,4-oxadiazole **9**, which affords the stereochemically rich and highly functionalized pentacyclic intermediate **8** as a single diastereomer in one step. The work extends the divergent total synthesis of four to now six different natural product alkaloid classes by distinguishing late stage key strategic bond formations within the underlying *Aspidosperma* core from the common intermediate **8**. Together, the work represents use of strategic bond analysis combined with the strategy of divergent synthesis to access six different natural product classes from a single intermediate.

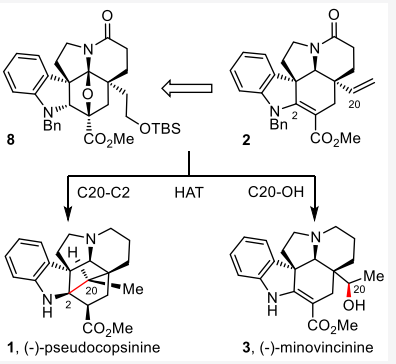

INTRODUCTION

(−)-Pseudocopsinine (**1**, aka pseudokopsinine) was first isolated in 1967 by Yunusov from *Vinca erecta* Regel et. Schmalh.[1] Later, its structure and absolute configuration were established by X-ray crystallography by Adrianov in 1974.[2] Related to the *Aspidosperma* alkaloids but containing an additional C20−C2 bond, the unique hexacyclic system of **1** features an unusual central strained bicyclo[2.2.1]heptane core and six contiguous stereocenters, of which three are quaternary and two are adjacent to one another. Prior synthetic efforts toward **1** are limited to the model studies of Penkett and Parsons[3,4] and semisyntheses of the related natural products tuboxenin[5] and vindolinine ($\Delta^{6,7}$-**1**) by Levy.[6] The latter employed a sodium-mediated radical cyclization of 20-iodotabersonine to effect C20−C2 bond formation without control of the relative stereochemistry, resulting in a mixture of all four possible C20/C3 diastereomers in a low combined yield of ca. 8%, of which $\Delta^{6,7}$-**1** was a minor component. Notably, a more traditional AIBN-initiated Bu_3SnH-mediated free radical reaction of the secondary radical onto a hindered tetrasubstituted and poor acceptor alkene failed to promote cyclization with bond formation adjacent to a quaternary carbon, resulting simply in iodide reduction.[6] Herein, we disclose the first total synthesis of **1** through late-stage formation of the strategic C20−C2 bond effected by an iron-mediated hydrogen atom transfer (HAT)[7,8] transannular radical cyclization of olefin **2** (Figure 1). Our focus on formation of the C20−C2 bond in spite of the largely failed precedent arises from the fact that it is a strategic bond, providing the greatest simplification of the target structure in a retrosynthetic analysis of **1**.[9] A metal-mediated HAT reaction, of which our early studies[7] served as a catalyst for its present day renaissance, was explored and successfully implemented based on insights detailed herein. To date, a metal-based HAT-mediated free radical cyclization has been implemented in less than 10 complex natural product total syntheses.[10,11] Only two constitute a more challenging and typically slower transannular cyclization,[10] of which one is reported to be inferior to a more traditional alkyl bromide/Bu_3SnH-mediated cyclization.[10b] The underlying *Aspidosperma* skeleton in **2** was accessed in a single step through the scalable tandem [4 + 2]/[3 + 2] cycloaddition cascade of acyclic precursor **9**, furnishing **8** in good yield and perfect diastereoselectivity.[12,13]

A bonus of this strategy is that it also permitted the first total synthesis of (−)-minovincinine (**3**) from the same intermediate **2**. Oxidation (O_2)[7,14] versus transannular cyclization of the HAT radical intermediate derived from **2** was used to form the C20−OH bond and access **3**. This *Aspidosperma* alkaloid was first isolated from *Vinca erecta* L. in 1962 by Janot,[15] and its C20 relative stereochemistry was established

Received: October 20, 2020

https://dx.doi.org/10.1021/acs.joc.0c02493
J. Org. Chem. XXXX, XXX, XXX−XXX

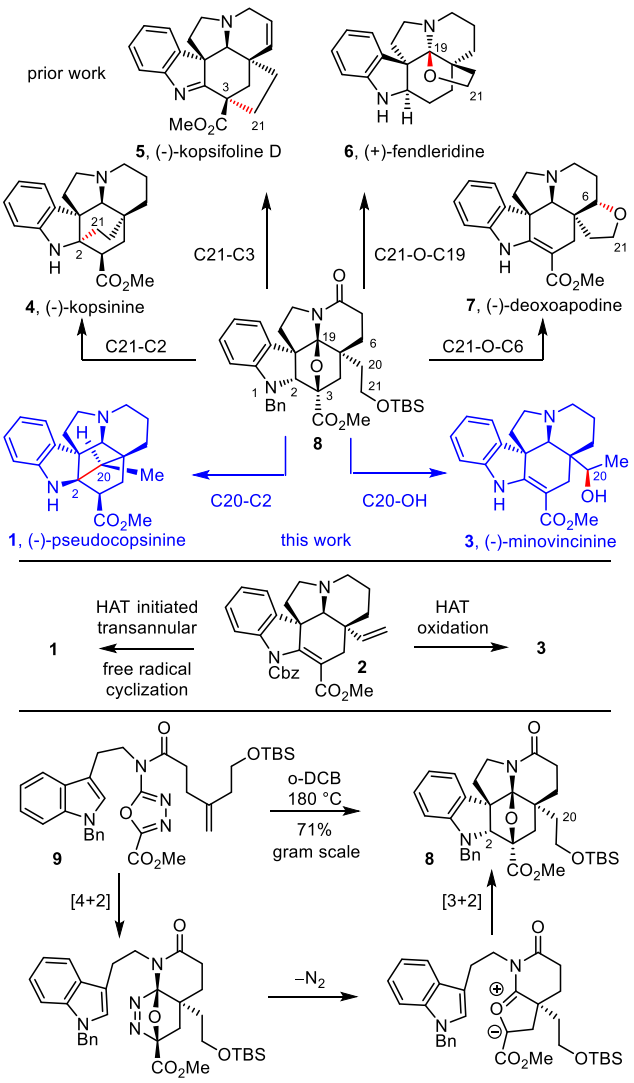

Figure 1. Late-stage strategic bond formation enables divergent syntheses of six natural product classes from key intermediate **8**, the product of a [4 + 2]/[3 + 2] cycloaddition cascade of **9**.

initially through Horeau's method (preferential acylation reactivity)[16] and recently supported by 2D-NMR analysis.[17] Minovincinine (**3**) has been the subject of biosynthetic studies[18−20] and one semisynthesis,[21] but no total synthesis of **3** has been reported to date. The efforts detailed herein represent the first total syntheses of **1** and **3**, both accessed from **8**, complementing our recent total syntheses of (−)-kopsinine (**4**),[22,23] (+)-fendleridine (**6**),[24] (−)-kopsifoline D (**5**), and (−)-deoxoapodine (**7**)[25] from the same common intermediate **8** (Figure 1). The prior studies enlisted the masked C21 alcohol in **8** as a synthetic handle for formation of the strategic C21−C2, C21−O−C19, C21−C3, and C21−O−C6 bonds, respectively. The total syntheses of **1** and **3** described herein shifts this functionalization site from C21 to C20 to access two new classes of alkaloids. Combined with earlier studies, these efforts now provide the divergent total syntheses[26] of six different alkaloid classes from the common intermediate (**8**), notably with late-stage strategic bond formation. Combined, the work represents use of strategic bond analysis[9] and the strategy of divergent synthesis[26] to access six different natural product classes from a common intermediate.

RESULTS AND DISCUSSION

Central to the assemblage of **8** was the [4 + 2]/[3 + 2] cycloaddition cascade of **9** (Figure 1), which was prepared in four steps from N-benzyltryptamine and 4-(2-*tert*-butyldimethylsilyloxy)pent-4-enoic acid, requiring only two purifications.[24] As detailed earlier,[24] warming a solution of **9** in *o*-dichlorobenzene (*o*-DCB) at 180 °C initiates an intramolecular [4 + 2] cycloaddition between the tethered alkene and 1,3,4-oxadiazole, which is followed by a loss of N_2 to generate a uniquely stabilized 1,3-dipole. This intermediate undergoes a subsequent [3 + 2] cycloaddition with the tethered indole with complete endo selectivity directed to the face opposite the newly formed lactam to give **8** as a single diastereomer (74−84%, gram-scale),[24b] a stereochemical outcome dictated by the linking tether. Diastereoselective reductive oxido bridge ring opening of **8** ($NaCNBH_3$, AcOH/iPrOH, 73%) with reduction of the intermediate *N*-acyliminium ion exclusively from the less hindered convex face provided alcohol **10** (Scheme 1).[22−25]

Scheme 1. Synthesis of (−)-14 from 8

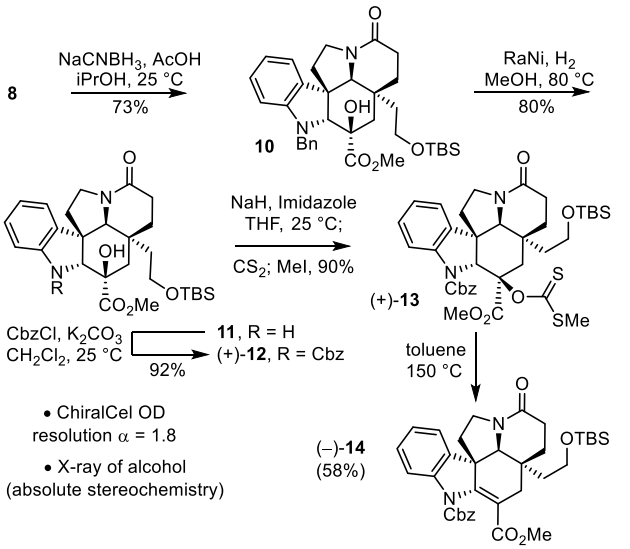

Compound **10** could be advanced to intermediate **14** by our previously reported sequence. In detail, debenzylation of **10** (Raney Ni, H_2, 80%) provided **11** that was converted to carbamate **12** (CbzCl, K_2CO_3, 92%). The enantiomers of **12** can be easily resolved chromatographically to give natural (+)-**12**, displaying a chromatographic a value of 1.8 (Chiralcel OD, 20% *i*-PrOH/hexanes) and providing an intermediate for which the absolute configuration was unambiguously assigned by X-ray.[22] In addition to providing a remarkably simple chromatographic resolution of **12**, the protecting group exchange also improved the regioselectivity of the subsequent Chugaev elimination of methyl xanthate (+)-**13**, which was prepared from (+)-**12** (NaH, CS_2; MeI, 90%). Heating a solution of (+)-**13** (toluene, 150 °C) afforded the tetrasubstituted olefin (−)-**14** (58%).[23]

(−)-Pseudocopsinine. With newly prepared (−)-**14** in hand, the studies commenced targeting olefin (−)-**2**. The amide of (−)-**14** was reduced selectively to the corresponding tertiary amine and subsequent acidic workup with in situ silyl ether deprotection afforded (−)-**15** (BH_3; 1 M aq. HCl, 83%). After surveying a range of methods for alcohol dehydration, a

https://dx.doi.org/10.1021/acs.joc.0c02493
J. Org. Chem. XXXX, XXX, XXX−XXX

selenoxide elimination[27] (Scheme 2) reported by Mukai and coworkers[28] was found to provide the olefin (−)-**2** from

Scheme 2. Synthesis of (−)-2 by Selenoxide Elimination

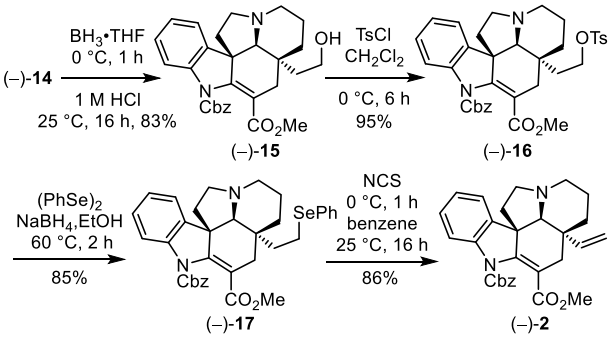

(−)-**15** in high yield. Thus, alcohol (−)-**15** was converted to tosylate (−)-**16** (TsCl, Et_3N, 95%), which was subsequently displaced by in situ generated PhSeNa to afford selenide (−)-**17**[29] ($NaBH_4$, $(PhSe)_2$, 85%). Treatment of (−)-**17** with N-chlorosuccinimide[30] (NCS) provided the corresponding selenoxide that underwent syn elimination at room temperature to afford (−)-**2** in 86% yield (69% overall from **15**), setting the stage for the HAT-initiated transannular free radical cyclization to the pseudocopsinine skeleton.

Initial efforts conducted with racemic material, which were inspired by the success of the dehydration of **12**, examined the Chugaev elimination (Scheme 3) for dehydration of (±)-**15**.

Scheme 3. Synthesis of (±)-2 by Chugaev Elimination

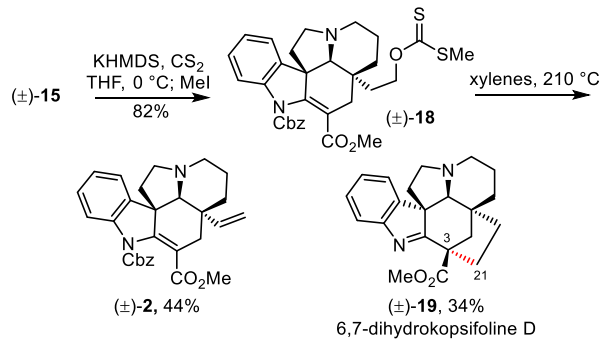

Use of typical conditions for formation of the methyl xanthate (CS_2, NaH, ImH; MeI) afforded (±)-**18** in poor and capricious yields (10−35%). However, stoichiometric deprotonation of (±)-**15** (KHMDS, 1 equiv) followed by sequential reaction with CS_2 and MeI afforded (±)-**18** reliably in good yield (82%). The methyl xanthate (±)-**18** underwent elimination in xylenes to afford olefin (±)-**2** in 44% yield, accompanied by a near-equal amount of (±)-**19** (34%), bearing the kopsifoline core (6,7-dihydro-kopsifoline D)[25] and arising through an intramolecular enamide displacement of the xanthate with Cbz cleavage. In efforts to increase selectivity for formation of (±)-**2**, the corresponding phenyl and benzyl xanthates of (±)-**18** were also examined and afforded similar results. Although the rates of elimination for both were twice as fast as the methyl xanthate (±)-**18** (see Supporting Information), the relative competitive formation of (±)-**2** and (±)-**19** proved essentially independent of the xanthate structure.

Gratifyingly, treatment of alkene (−)-**2** with phenylsilane ($PhSiH_3$) in the presence of $Fe(acac)_3$[8] (Scheme 4) provided

Scheme 4. HAT-Initiated Transannular Free Radical Cyclization of (−)-2

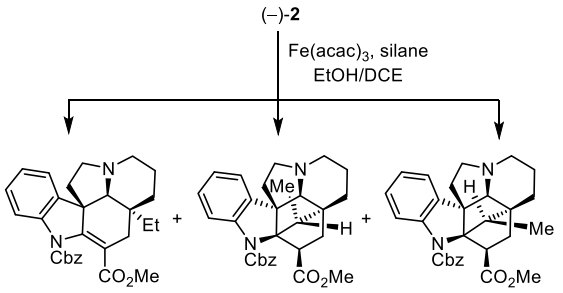

Conditions	(−)-22	(−)-21	(−)-20	(−)-2
$Fe(acac)_3$ (1.5 equiv) $PhSiH_3$ (5 equiv) EtOH/$(CH_2Cl)_2$ (9:1, 3 mM)* 25 °C, 16 h	60%	20%	7%	10%

*Subjected to 3 cycles of freeze-pump-thaw

- Generation and reaction of secondary radical adjacent to quaternary center
- Transannular cyclization onto a tetrasubstituted and poor acceptor alkene
- Formation of strained [2.2.1] ring system and quaternary center adjacent to yet another quaternary center

the desired transannular cyclization reaction in excellent yield (80%) and good diastereoselectivity (3:1), favoring formation of the desired diastereomer (−)-**22** (60%) as well as a minor amount of the alkene reduction product (−)-**20** (7%) and a small amount of recovered (−)-**2** (10%) (Scheme 4).

Notably, the reaction provided a 3:1 diastereoselectivity for formation of the C20 center and exclusive diastereoselectivity for formation of the C3 center. The yield of cyclization increased with increasing $Fe(acac)_3$ (1.5 vs 0.5 equiv) and time (16 vs 2 h) and decreased relative to reduction with use of a stronger reductant ($PhSiH_2(OiPr)$[31] vs $PhSiH_3$), see Supporting Information. In addition, the cyclization diastereoselectivity for generation of the desired diastereomer (−)-**22** versus (−)-**21** increased with decreasing reaction temperature (25 vs 50 °C).

It is a remarkable result given the ring strain introduced with the cyclization, the poor acceptor alkene and its tetrasubstitution, the hindered nature of the reacting secondary radical located adjacent to a quaternary center, and bond formation to generate a quaternary center adjacent to yet another quaternary center. Key to the success of the HAT-mediated transannular cyclization relative to more traditional methods (e.g., Bu_3SnH) can be attributed to slow, low level Fe(III)−H generation (25 °C) with use of a weak reductant ($PhSiH_3$), both of which minimize intermediate radical reduction. It is also plausible that the released Fe(II) reacts with and stabilizes the initially formed C20 radical through reversible formation of a C20−Fe(III) bond[14,32] that slows or prevents its reduction before desired cyclization and where the adjacent C5 quaternary center prevents olefin isomerization[8b] through counterproductive Fe(III)−H elimination in competition with the slow cyclization. It is even plausible, and our studies do not rule out, that an intermediate C20 Fe species coordinates the acceptor alkene and undergoes direct carbometalation.

https://dx.doi.org/10.1021/acs.joc.0c02493
J. Org. Chem. XXXX, XXX, XXX−XXX

The diastereoselectivity for preferential formation of **22** can be rationalized based on the mechanistic studies of Holland and coworkers[32] (Scheme 5). Markovnikov hydrogen atom transfer to **2** first generates radical **A** by way of an in situ generated Fe(III) hydride. The free radical intermediate undergoes an irreversible and kinetically controlled conjugate addition through two competing transition states (**TS-21.1** and **TS-22.1**). In the more favorable transition state **TS-22.1**, the C20 methyl group avoids the 1,3-steric repulsion of the C19 and C6 hydrogen atoms and that of the C12 aryl substituent that disfavors the more sterically congested **TS-21.1**, preferentially providing the desired C20 stereochemistry. Both **TS-21.1** and **TS-22.1** yield the corresponding C3 radicals that are either quenched by free radical hydrogen atom abstraction or further reduced by Fe(II) to provide the intermediate enolates. Either enolate protonation or the hydrogen atom reduction occurs exclusively from the sterically less congested convex face for both C20 diastereomers to give (−)-**21** and (−)-**22** in 20 and 60%, respectively.

Scheme 5. Rationale for Diastereoselectivity of the Transannular Free Radical Cyclization of (−)-2

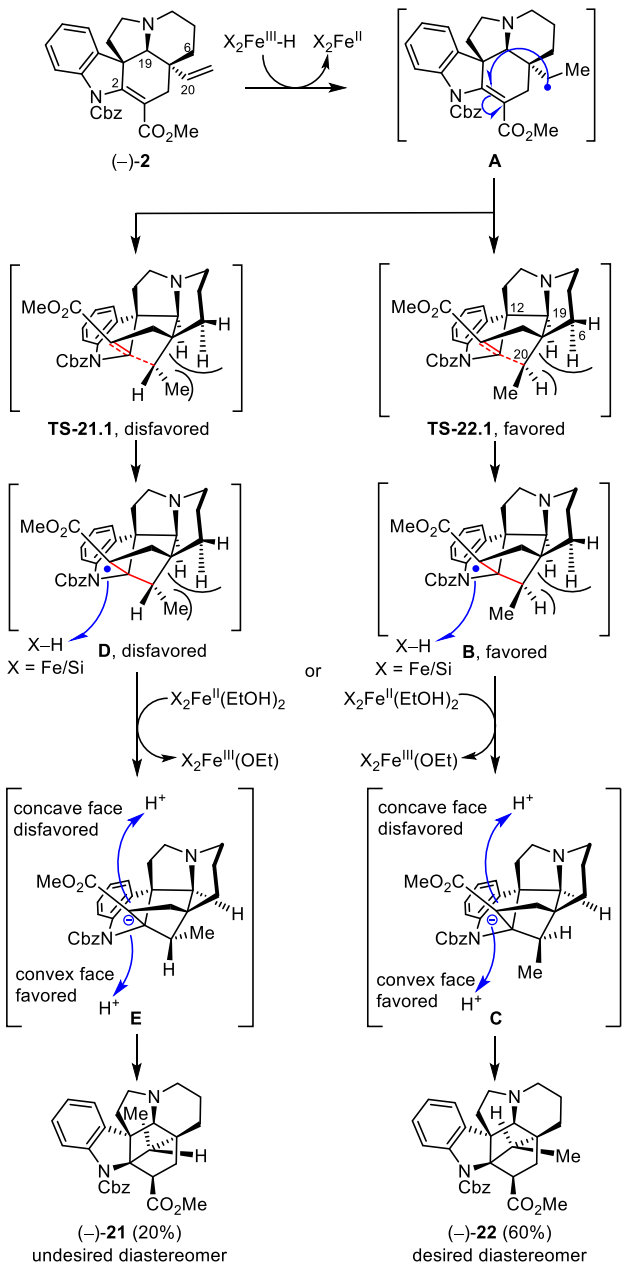

Without optimization, Cbz removal from (−)-**22** (Pd/C, H_2, 64%) and (−)-**21** (Pd/C, H_2, 58%) completed the total synthesis of (−)-**1** ($[\alpha]_D^{22}$ −23 (*c* 0.075, MeOH), reported $[\alpha]_D$ −30 (*c* 1.5, MeOH)[33]) and 20-epi-**1** ($[\alpha]_D^{25}$ −7.5 ± 0.2 (*c* 0.33, MeOH), respectively (Scheme 6). The ^{13}C NMR chemical shifts of synthetic **1** matched closely those reported by Yagudaev[33] and Janot[34] for **1** (Supporting Information Table S1). Unambiguous confirmation of the synthesis of pseudocopsinine (**1**) was established by X-ray crystallography conducted on the hydrochloride salt of **1** with determination of the relative stereochemistry of synthetic **1**.[35] This latter result, matching the X-ray of the natural product, resolves a disparity raised by the subtle differences in the ^{13}C NMR spectra recorded by Yagudaev[33] and Janot,[34] which match ours well, and earlier spectra (see SI Table S1). It is not the structure assignment that is in question, rather simply the result of an understandable less accurate recording of the spectra in the early days of ^{13}C NMR.[33]

Scheme 6. Completion of the Total Syntheses of 1 and 20-epi-1

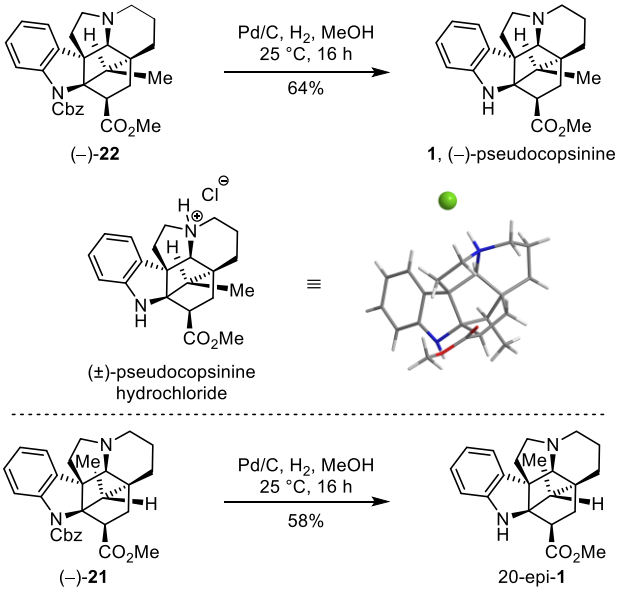

(−)-Minovincinine. An additional attribute of the approach is that this same intermediate (−)-**2** allowed for the divergent synthesis of (−)-minovincinine. To introduce the C20 hydroxyl group (Scheme 7), (−)-**2** was subjected to a series of HAT-initiated oxidation conditions for alcohol introduction[14] and representative results are summarized in Scheme 7. Optimized conditions (Scheme 7, entry 1) afforded a near 1:1 mixture (82%) of the desired diastereomer (−)-**24** and its isomer (−)-**23**. Interestingly, the classical Mukaiyama hydration conditions (Scheme 7, entry 3) gave **25** as a single diastereomer exclusively (see the Supporting Information), which upon reduction with $NaCNBH_3$ provided exclusively **23**. Replacement of $Co(acac)_2$ with Co complex **A**[36] suppressed formation of **25** and provided a modest 34% yield of olefin hydration (Scheme 7, entry 2) with a 2.5:1 preference for the desired diastereomer (−)-**24**. Although not investigated in

https://dx.doi.org/10.1021/acs.joc.0c02493
J. Org. Chem. XXXX, XXX, XXX−XXX

Scheme 7. HAT-Mediated Oxidation of (−)-2

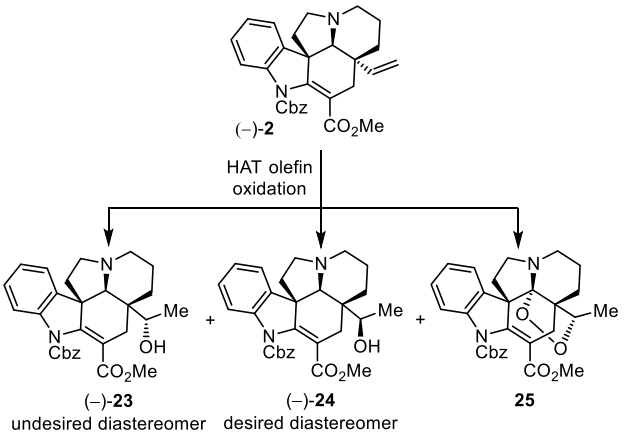

Entry	Conditions	(−)-23	(−)-24	25
1	**B**, $PhSiH_3$, O_2 EtOH, 25 °C, 16 h	44%	38%	0%
2	**A**, $PhSiH_3$, O_2 EtOH, 25 °C, 16 h	10%	24%	23%
3	$Co(acac)_2$, $PhSiH_3$ EtOH, O_2, 25 °C, 16 h	0%	0%	90%
4	Fe(pthalocyanine) $NaBH_4$, O_2, EtOH 0°C to 25 °C, 16 h	24%	14%	0%
5	$Fe_2(ox)_3$, $NaBH_4$ O_2, TFE:H_2O:HCl 0°C to 25 °C, 16 h	17%	14%	0%
6	$Mn(acac)_3$ $PhSiH_2(OiPr)$ THF, O_2, 50 °C, 1h	23%	25%	0%

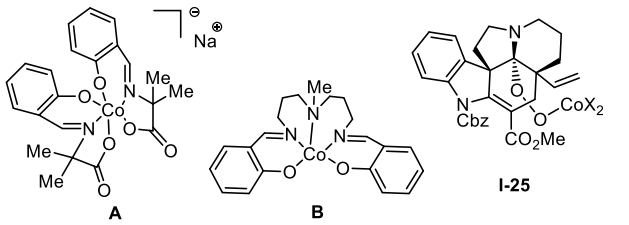

detail, it is likely that C19 oxidation prior to olefin oxidation, perhaps to an iminium radical cation, followed by oxygen or peroxide attack[37,38] to form a Co(III) peroxide intermediate such as **I-25**[39,40] is responsible for formation of **25**, accounting for the single diastereomer formed.[41] The use of FePc and $Fe_2(ox)_3$[7] (Scheme 7, entries 4 and 5), $Mn(acac)_3$[31] (Scheme 7, entry 6), as well as $Fe(NO_3)_3$, $Fe_2(SO_4)_3$, $Fe(acac)_3$, $Fe(dpm)_3$, and $Mn(dpm)_3$ (not shown) gave low yields of alkene hydration.

Removal of the Cbz group from (−)-**23** (PtO_2, H_2, 89%) and (−)-**24** (PtO_2, H_2, 99%) afforded 20-epi-**3** ($[\alpha]_D^{25}$ −429 (*c* 0.07, MeOH) and (−)-**3** ($[\alpha]_D^{25}$ −497 ± 1 (*c* 0.07, MeOH), reported $[\alpha]_D^{20}$ −514 (*c* 0.07, EtOH)[17]), respectively (Scheme 8), and the latter displayed an ^1H NMR identical with that reported for the natural isolate[14] (Supporting Information).

CONCLUSIONS

The first total syntheses of (−)-pseudocopsinine and (−)-minovincinine detailed herein were achieved in a divergent synthesis from a common intermediate **8** with late stage strategic bond formation or functionalization unique to their cores or structure. The approach features two metal-mediated HAT reactions of the intermediate olefin **2**, effecting a transannular C20−C2 free radical cyclization of a challenging

Scheme 8. Completion of Total Syntheses of 3 and 20-epi-3

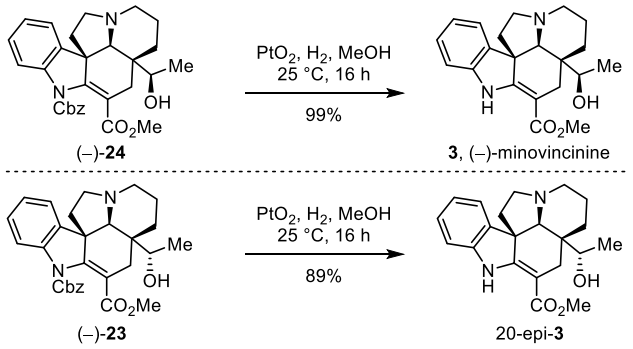

substrate with formation of a strained [2.2.1] ring system employing a poor tetrasubstituted acceptor alkene and hindered secondary free radical (for **1**), or a Markovnikov free radical oxidation reaction (for **3**). These efforts complement our previous total syntheses of (−)-kopsinine (**4**), (+)-fendleridine (**6**), (−)-kopsifoline D (**5**), and (−)-deoxoapodine (**7**), culminating in a total of six syntheses of natural products belonging to different alkaloid classes from the same common intermediate **8**. Central to assemblage of the common intermediate **8** is the powerful intramolecular [4 + 2]/[3 + 2] cascade of a 1,3,4-oxadiazole that provided the underlying densely functionalized pentacyclic core as a single diastereomer in one step from a simple linear precursor. The preprogrammed oxidation at C21 was subsequently and efficiently relayed to C20, permitting access to both (−)-pseudocopsinine and (−)-minovincinine.

EXPERIMENTAL SECTION

General Methods. Unless otherwise stated, all reactions were performed in oven-dried or flame-dried glass round-bottom flasks with a rubber septum or Fisher brand borosilicate glass reaction tubes with a black phenolic screw cap under an atmosphere of dry nitrogen or argon. All reactions that require heating used an oil bath as the heat source. All reagents and solvents were purchased from either Fischer Chemical or Millipore-Aldrich and used directly without further purification. Preparative TLC (PTLC) and column chromatography were conducted using Millipore SiO_2 60 F254 PTLC (0.5 mm) and Zeochem ZEOprep 60 ECO SiO_2 (40−63 μm), respectively. Volatile solvents were removed under reduced pressure using a rotary evaporator. IR spectra were obtained using a Thermo Nicolet 380 FT-IR with a SmartOrbit Diamond ATR accessory. High resolution mass spectrometry (HRMS) analysis was performed by direct sample injection on an Agilent G1969A ESI-TOF mass spectrometer. The single crystal X-ray diffraction studies were carried out on a Bruker Kappa APEX-II CCD diffractometer equipped with Mo Kα radiation (λ = 0.71073) at the UCSD Crystallography Facility. Structural assignments were made with additional information from gCOSY, gHSQC, gNOESY, and gHMBC experiments.

(−)-15. A stirred solution of (−)-**14**[22] (351 mg, 0.569 mmol) in anhydrous THF (50 mL) under Ar at 0 °C was treated with BH_3·THF (1 M in THF, 8.5 mL, 8.5 mmol) and was stirred at 0 °C until full conversion (1 h). The reaction mixture was quenched with addition of distilled water until gas evolution ceased (1 mL added), followed by addition of 40 mL of aqueous 1 M HCl. The resulting solution was removed from the cold bath and stirred for 16 h at 25 °C. The mixture was basified to pH 8 with addition of aqueous 1 M NaOH (22 mL) and extracted with EtOAc (3 × 50 mL). The combined organic layers were dried over $MgSO_4$ and concentrated under reduced pressure. Flash chromatography (SiO_2, 40% EtOAc/hexane) afforded (−)-**15** (227 mg, 83%) as white foam. ^1H NMR (600 MHz, $CDCl_3$) δ 7.77−7.71 (m, 1H), 7.39−7.29 (m, 5H), 7.21 (td, *J* = 7.7, 1.3 Hz, 1H), 7.16 (dd, *J* = 7.4, 1.3 Hz, 1H), 7.03 (td, *J* =

https://dx.doi.org/10.1021/acs.joc.0c02493
J. Org. Chem. XXXX, XXX, XXX−XXX

7.5, 1.1 Hz, 1H), 5.36 (d, J = 12.4 Hz, 1H), 5.13 (d, J = 12.4 Hz, 1H), 3.53 (s, 3H), 3.52−3.43 (m, 2H), 3.12 (ddt, J = 10.8, 4.2, 1.9 Hz, 1H), 3.07 (d, J = 15.2 Hz, 1H), 2.93−2.86 (m, 1H), 2.41−2.33 (m, 2H), 2.27 (td, J = 11.2, 2.9 Hz, 1H), 2.17 (td, J = 11.7, 7.1 Hz, 1H), 2.08 (dd, J = 15.3, 1.9 Hz, 1H), 1.91−1.80 (m, 2H), 1.64 (dd, J = 12.0, 5.5 Hz, 1H), 1.58 (ddd, J = 13.4, 6.2, 2.9 Hz, 1H), 1.44−1.31 (m, 2H), 0.94 (ddd, J = 13.5, 7.5, 5.8 Hz, 2H); $^{13}C\{^1H\}$ NMR (151 MHz, $CDCl_3$) δ 168.1, 152.5, 149.6, 140.3, 138.1, 135.9, 128.7, 128.3, 128.2, 127.7, 124.1, 120.6, 115.9, 112.6, 71.0, 68.0, 58.6, 53.4, 51.8, 51.8, 51.6, 42.8, 39.3, 37.3, 33.9, 28.8, 22.3; IR (film) ν_{max} 3433, 2933, 2778, 1717, 1473, 1391, 1356, 1328, 1303, 1282, 1253, 1215, 1180, 1126, 1068, 1045, 905, 851, 752, 697 cm^{-1}; HRMS (ESI-TOF) m/z 489.2376 $[(M + H)^+$, $C_{29}H_{33}N_2O_5^+$ requires 489.2389]; $[\alpha]_D^{23}$ −85 (c 0.61, $CHCl_3$).

(−)-16. A stirred solution of (−)-**15** (213 mg, 0.436 mmol) in CH_2Cl_2 (10 mL) was cooled to 0 °C and treated with Et_3N (3.30 mL, 23.7 mmol) followed by TsCl (997 mg, 5.23 mmol), and the reaction mixture was warmed to 25 °C and stirred for 6 h. The resulting solution was poured into H_2O (15 mL) and the organic layer was separated. The aqueous layer was extracted with CH_2Cl_2 (3 × 10 mL). The combined organic layers were dried over $MgSO_4$ and concentrated under reduced pressure. Flash column chromatography (SiO_2, 30% EtOAc/hexane) afforded (−)-**16** (267 mg, 95%) as white foam. ^1H NMR (600 MHz $CDCl_3$) δ 7.75 (d, J = 8.0 Hz, 1H), 7.64 (d, J = 8.1 Hz, 2H), 7.41−7.29 (m, 5H), 7.27 (d, J = 8.1 Hz, 2H), 7.21 (td, J = 7.8, 1.3 Hz, 1H), 7.11−7.07 (m, 1H), 7.01 (td, J = 7.5, 1.0 Hz, 1H), 5.35 (d, J = 12.3 Hz, 1H), 5.13 (d, J = 12.3 Hz, 1H), 3.83 (td, J = 6.6, 2.8 Hz, 2H), 3.52 (s, 3H), 3.08 (m, 2H), 2.88 (t, J = 7.8 Hz, 1H), 2.41 (s, 3H), 2.35 (ddd, J = 11.6, 8.6, 5.6 Hz, 1H), 2.31 (s, 1H), 2.27−2.20 (m, 1H), 2.15 (td, J = 11.6, 7.1 Hz, 1H), 2.00 (dd, J = 15.5, 1.9 Hz, 1H), 1.8−1.78 (m, 1H), 1.74 (d, J = 14.0 Hz, 1H), 1.62 (dd, J = 12.0, 5.5 Hz, 1H), 1.55 (m, 1H), 1.47 (dt, J = 14.2, 6.9 Hz, 1H), 1.29 (td, J = 13.6, 5.0 Hz, 1H), 1.01 (dt, J = 13.8, 6.3 Hz, 1H); $^{13}C\{^1H\}$ NMR (151 MHz, $CDCl_3$) δ 167.5, 152.4, 149.8, 144.7, 140.3, 137.6, 135.8, 132.9, 129.9, 128.7, 128.4, 128.2, 128.0, 127.7, 124.1, 120.6, 115.9, 112.1, 70.7, 68.0, 66.8, 53.4, 51.7, 51.6, 51.6, 42.7, 37.3, 34.9, 33.5, 28.5, 22.2, 21.8; IR (film) ν_{max} 2932, 2779, 1721, 1601, 1473, 1460, 1391, 1358, 1330, 1303, 1282, 1232, 1177, 0097, 1047, 1019, 952, 908, 874, 814, 753, 698, 664 cm^{-1}; HRMS (ESI-TOF) m/z 643.2482 $[(M + H)^+$, $C_{36}H_{39}N_2O_7S^+$, required 643.2478]; $[\alpha]_D^{22}$ −51 (c 0.39, $CHCl_3$).

(−)-17. A solution of (−)-**16** (267 mg, 0.416 mmol) in EtOH (15 mL) was cooled to 0 °C and treated with diphenyl diselenide (649 mg, 2.08 mmol). A solution of $NaBH_4$ (157 mg, 4.16 mmol) in EtOH (10 mL) was added to the reaction mixture dropwise, which then was warmed slowly to 25 °C over 30 min and subsequently warmed at 60 °C for 40 min. The reaction mixture was cooled to 25 °C and concentrated under reduced pressure. The crude residue was purified by flash column chromatography (SiO_2, 20% EtOAc/hexane) to afford (−)-**17** (223 mg, 85%) as white foam. ^1H NMR (600 MHz, $CDCl_3$) δ 7.73 (d, J = 8.0 Hz, 1H), 7.42−7.29 (m, 6H), 7.20 (t, J = 7.8 Hz, 1H), 7.15−7.08 (m, 5H), 7.01 (t, J = 7.5 Hz, 1H), 5.36 (d, J = 12.3 Hz, 1H), 5.13 (d, J = 12.3 Hz, 1H), 3.49 (s, 3H), 3.10 (d, J = 10.9 Hz, 1H), 3.02 (d, J = 15.5 Hz, 1H), 2.88 (t, J = 7.8 Hz, 1H), 2.64 (td, J = 12.1, 4.5 Hz, 1H), 2.52 (td, J = 12.0, 5.2 Hz, 1H), 2.40−2.31 (m, 2H), 2.28−2.21 (m, 1H), 2.14 (td, J = 11.6, 7.1 Hz, 1H), 2.04 (d, J = 15.1 Hz, 1H), 1.82 (dd, J = 28.9, 13.6 Hz, 2H), 1.65−1.60 (m, 2H), 1.47 (td, J = 13.4, 13.0, 5.1 Hz, 1H), 1.32 (td, J = 13.4, 13.0, 4.6 Hz, 1H), 1.12 (td, J = 13.4, 12.9, 4.4 Hz, 1H); $^{13}C\{^1H\}$ NMR (151 MHz, $CDCl_3$) δ 167.6, 152.5, 150.5, 140.3, 137.7, 135.9, 132.4, 129.8, 129.0, 128.7, 128.4, 128.2, 127.6, 126.8, 124.1, 120.5, 115.9, 111.9, 70.4, 68.0, 53.4, 51.8, 51.7, 51.5, 42.7, 39.0, 37.6, 33.5, 28.3, 22.3, 21.4; IR (film) ν_{max} 2931, 2787, 1721, 1474, 1436, 1391, 1356, 1328, 1303, 1281, 1250, 1231, 1200, 1181, 1157, 1116, 1068, 1047, 1019, 735, 694 cm^{-1}; HRMS (ESI-TOF) m/z 623.1966 $[(M + H)^+$, $C_{35}H_{37}N_2O_4{}^{74}Se^+$, required 623.1978] and m/z 629.1930 $[(M + H)^+$, $C_{35}H_{37}N_2O_4{}^{80}Se^+$, required 629.1919]; $[\alpha]_D^{22}$ −79 (c 0.54, $CHCl_3$).

(−)-2. A solution of (−)-**17** (223 mg, 0.355 mmol) in MeOH (10 mL) and CH_2Cl_2 (10 mL) was cooled to 0 °C and treated with a solution of NCS (47.4 mg, 0.355 mmol) in MeOH (1 mL) and CH_2Cl_2 (1 mL) dropwise. The reaction mixture was stirred at 0 °C for 40 min before being quenched with the addition of saturated aqueous $NaHCO_3$ (7 mL). The biphasic mixture was separated, and the aqueous layer was extracted with CH_2Cl_2 (3 × 40 mL). The combined organic layers were dried over $MgSO_4$, concentrated under reduced pressure, and the resulting residue was dissolved in benzene and left at 25 °C for 16 h. The resulting light-yellow solution was concentrated under reduced pressure, and the crude residue was subjected to flash column chromatography (SiO_2, 30% EtOAc/hexane) and afforded (−)-**2** (144 mg, 86%) as a white foam. ^1H NMR (600 MHz, $CDCl_3$) δ 7.72 (dt, J = 8.0, 0.7 Hz, 1H), 7.38−7.29 (m, 5H), 7.22−7.15 (m, 2H), 7.03 (td, J = 7.5, 1.1 Hz, 1H), 5.41 (dd, J = 17.9, 10.9 Hz, 1H), 5.35 (d, J = 12.3 Hz, 1H), 5.12 (d, J = 12.3 Hz, 1H), 4.73−4.68 (m, 2H), 3.54 (s, 3H), 3.19 (d, J = 15.1 Hz, 1H), 3.16−3.11 (m, 1H), 2.93 (dd, J = 8.6, 7.1 Hz, 1H), 2.63 (d, J = 1.8 Hz, 1H), 2.43 (ddd, J = 11.4, 8.6, 5.6 Hz, 1H), 2.35−2.27 (m, 1H), 2.23−2.11 (m, 2H), 1.88 (tdt, J = 13.4, 12.0, 4.6 Hz, 1H), 1.71−1.64 (m, 2H), 1.61 (ddd, J = 13.3, 5.1, 2.5 Hz, 1H), 1.46 (td, J = 13.7, 4.9 Hz, 1H);$^{13}C\{^1H\}$ NMR (151 MHz, $CDCl_3$) δ 167.9, 152.5, 150.2, 143.6, 140.4, 137.9, 135.9, 128.7, 128.3, 128.2, 127.5, 124.0, 120.6, 115.8, 113.9, 113.3, 69.9, 66.8, 53.7, 51.8, 51.6, 51.5, 42.9, 41.7, 35.2, 30.2, 22.1.; IR (film) ν_{max} 2935, 2776, 1722, 1603, 1473, 1461, 1435, 1390, 1356, 1326, 1302, 1281, 1251, 1231, 1204, 1182, 1120, 1050, 914, 751, 697 cm^{-1}; HRMS (ESI-TOF) m/z 471.2283 $[(M + H)^+$, $C_{29}H_{31}N_2O_4^+$, required 471.2284]; $[\alpha]_D^{21}$ −114 (c 0.48, $CHCl_3$).

(−)-22. A solution of (−)-**2** (20 mg, 0.042 mmol) and $Fe(acac)_3$ (22.5 mg, 0.0637 mmol) in EtOH (12.5 mL) was subjected to 3 cycles of freeze−pump−thaw and placed under Ar before being treated with a solution of phenylsilane in dichloroethane (0.15 M, 1.4 mL, 0.21 mmol, subjected to 3 cycles of freeze−pump−thaw) at 25 °C under Ar. The reaction mixture was stirred 25 °C for 16 h before being quenched by the addition of a mixture of saturated aqueous $NaHCO_3$, saturated aqueous Rochelle's salt, and saturated aqueous $Na_2S_2O_4$ (1:1:1, v/v, 10 mL). The resulting biphasic mixture was stirred vigorously for 30 min at 25 °C under open air, which was then extracted with EtOAc (3 × 10 mL). The combined organic layers were dried over $MgSO_4$ then concentrated under reduced pressure, and the resulting crude residue was purified by PTLC (SiO_2, 50% acetone/hexane, developed 3 times) to afford recovered (−)-**2** (2.1 mg, 10%, R_f: 0.9), (−)-**20** (1.4 mg, 7%, R_f: 0.8), the desired diastereomer (−)-**22** (11.8 mg, 60%, R_f: 0.5) and undesired diastereomer (−)-**21** (4.0 mg, 20%, R_f: 0.45) as white powders. For (−)-**20**: ^1H NMR (600 MHz, $CDCl_3$) δ 7.75 (d, J = 8.0 Hz, 1H), 7.40−7.29 (m, 5H), 7.20 (td, J = 7.8, 1.3 Hz, 1H), 7.16 (d, J = 7.3 Hz, 1H), 7.03 (t, J = 7.5 Hz, 1H), 5.36 (d, J = 12.3 Hz, 1H), 5.13 (d, J = 12.3 Hz, 1H), 3.54 (s, 3H), 3.12 (d, J = 11.0 Hz, 1H), 2.98 (d, J = 15.3 Hz, 1H), 2.93−2.86 (m, 1H), 2.39−2.33 (m, 2H), 2.25 (td, J = 11.3, 2.8 Hz, 1H), 2.21−2.14 (m, 1H), 2.02 (dd, J = 15.4, 1.8 Hz, 1H), 1.90−1.81 (m, 1H), 1.76 (d, J = 13.8 Hz, 1H), 1.63 (dd, J = 12.0, 5.6 Hz, 1H), 1.59 (m, 1H), 1.23 (dd, J = 13.5, 4.9 Hz, 1H), 1.15−1.06 (m, 1H), 0.70 (dq, J = 14.3, 7.3 Hz, 1H), 0.56 (t, J = 7.5 Hz, 3H); $^{13}C\{^1H\}$ NMR (151 MHz, $CDCl_3$) δ 167.9, 152.5, 150.0, 140.4, 138.4, 135.9, 128.7, 128.3, 128.2, 127.5, 123.9, 120.6, 115.8, 112.5, 71.1, 67.9, 53.4, 51.9, 51.9, 51.5, 42.7, 38.0, 32.9, 29.0, 28.0, 22.4, 7.3; IR (film) ν_{max} 2931, 2776, 1722, 1473, 1460, 1391, 1356, 1328, 1303, 1280, 1250, 1231, 1183, 1114, 1049, 1019, 752, 698, 623 cm^{-1}; HRMS (ESI-TOF) m/z 473.2443 $[(M + H)^+$, $C_{29}H_{33}N_2O_4^+$, required 473.2440]; $[\alpha]_D^{20}$ −44 (c 0.14, $CHCl_3$). For (−)-**21**: ^1H NMR (500 MHz, DMSO-d_6, 55 °C) δ 7.69 (s, 1H), 7.49−7.33 (m, 5H), 7.22−7.12 (m, 2H), 7.01 (t, J = 7.6 Hz, 1H), 5.32 (s, 2H), 3.99 (s, 1H), 3.51 (s, 3H), 3.25 (s, 2H), 3.12 (s, 1H), 3.02 (d, J = 12.1 Hz, 1H), 2.92 (d, J = 11.0 Hz, 1H), 2.79 (dd, J = 13.9, 6.4 Hz, 1H), 2.33 (s, 1H), 2.23−2.07 (m, 1H), 1.69 (d, J = 12.9 Hz, 2H), 1.62−1.46 (m, 3H), 1.42 (s, 1H), 0.36 (d, J = 7.2 Hz, 3H); $^{13}C\{^1H\}$ NMR (126 MHz, DMSO-d_6, 55 °C) δ 173.2, 152.4, 138.3, 136.2, 128.2, 127.8, 127.7, 127.2, 123.3, 121.4, 113.8, 79.8, 75.7, 66.3, 57.8, 55.0, 53.5, 51.2, 47.0, 42.7, 32.5, 28.2, 20.5, 9.1; IR (film) ν_{max} 2938, 1705, 1599, 1480, 1459, 1398, 1350, 1325, 1255, 1219, 1204, 1155, 1130, 1102, 1040, 1023, 753, 699, 618 cm^{-1}; HRMS (ESI-TOF) m/z 473.2441 $[(M + H)^+$, $C_{29}H_{33}N_2O_4^+$, required 473.2440]; $[\alpha]_D^{21}$ −50 (c 0.40,

https://dx.doi.org/10.1021/acs.joc.0c02493
J. Org. Chem. XXXX, XXX, XXX−XXX

$CHCl_3$). For (−)-**22**: ^{1}H NMR (500 MHz, DMSO-d_6, 70 °C) δ 7.66 (s, 1H), 7.46−7.30 (m, 5H), 7.23 (dd, J = 7.5, 1.4 Hz, 1H), 7.19−7.13 (m, 1H), 7.02 (td, J = 7.4, 1.1 Hz, 1H), 5.24 (s, 2H), 4.20 (s, 1H), 3.48 (s, 3H), 3.18 (dt, J = 8.4, 6.5 Hz, 1H), 3.15−3.00 (m, 2H), 2.91−2.80 (m, 2H), 2.74 (ddd, J = 14.4, 6.8, 1.8 Hz, 1H), 2.12−2.04 (m, 1H), 1.81−1.70 (m, 2H), 1.69−1.49 (m, 3H), 1.48−1.33 (m, 2H), 0.90 (d, J = 6.8 Hz, 3H); ^{13}C{^{1}H} NMR (126 MHz, DMSO-d_6, 70 °C) δ 173.6, 152.6, 141.1, 138.7, 135.9, 128.0, 127.9, 127.7, 126.8, 123.2, 122.5, 115.2, 80.1, 79.2, 66.3, 58.9, 53.8, 52.0, 50.9, 47.5, 43.5, 37.9, 29.4, 28.2, 20.1, 13.3, 8.1; IR (film) ν_{max} 2935, 1705, 1480, 1461, 1399, 1349, 1324, 1292, 1219, 1153, 1106, 1047, 752, 698, 643 cm^{-1}; HRMS (ESI-TOF) m/z 473.2445 [(M + H)$^+$, $C_{29}H_{33}N_2O_4^+$, required 473.2440]; $[\alpha]_D^{21}$ −53 (c 1.18, $CHCl_3$).

(−)-Pseudocopsinine ((−)-1). Pd/C (10% Pd w/w, 4.5 mg, 0.0042 mmol) was suspended in a solution of (−)-**22** (4.0 mg, 0.0085 mmol) in MeOH (2 mL). The suspension was sparged with H_2 gas for 20 min while vigorously stirring at 25 °C before being stirred for 16 h at 25 °C under a H_2 atmosphere. The reaction mixture was filtered through Celite, and the filtrate was concentrated under reduced pressure. The residue was purified by PTLC (SiO_2, 5% MeOH/CH_2Cl_2) to afford (−)-pseudocopsinine (**1**, 1.9 mg, 64%). ^{1}H NMR (600 MHz, $CDCl_3$) δ 7.27 (s, 1H), 7.06 (td, J = 7.6, 1.3 Hz, 1H), 6.85 (td, J = 7.4, 1.0 Hz, 1H), 6.80−6.76 (m, 1H), 3.70 (s, 3H), 3.33 (td, J = 8.9, 6.8 Hz, 1H), 3.19 (m, 2H), 3.14−3.08 (m, 1H), 3.05 (dq, J = 11.8, 6.2, 5.6 Hz, 2H), 2.87 (ddd, J = 14.3, 6.3, 2.1 Hz, 1H), 2.12 (ddd, J = 14.7, 6.7, 2.8 Hz, 1H), 1.84−1.68 (m, 4H), 1.57 (qd, J = 9.1, 4.5 Hz, 2H), 1.52−1.45 (m, 1H), 0.85 (d, J = 6.7 Hz, 3H); ^{13}C{^{1}H} NMR (151 MHz, $CDCl_3$) δ 175.2, 149.6, 140.2, 127.4, 123.8, 121.4, 112.9, 80.6, 78.7, 60.4, 55.1, 52.1, 51.1, 48.1, 44.6, 40.3, 37.3, 31.3, 29.0, 20.6, 7.6; IR (film) ν_{max} 3369, 2931, 1725, 1607, 1464, 1435, 1375, 1347, 1322, 1203, 1132, 1102, 1074, 950, 889, 746, 699, 669, 651 cm^{-1}; HRMS (ESI-TOF) m/z 339.2077 [(M + H)$^+$, $C_{21}H_{27}N_2O_2^+$, required 339.2073]; $[\alpha]_D^{25}$ −5.5 (c 1.5, $CHCl_3$) and $[\alpha]_D^{25}$ −23.4 (c 0.075, MeOH), Yagudaev[33] reported $[\boldsymbol{\alpha}]_D$ −30.4 (c 1.51, MeOH).

(±)-Pseudocopsinine Hydrochloride ((±)-1·HCl). A solution of (±)-pseudocopsinine (4.6 mg, 0.014 mmol, prepared by the route above with racemic material) in EtOH (0.2 mL) at 0 °C was treated with ethanolic HCl (0.42 M, 0.16 mL) and warmed slowly to 25 °C. The reaction solvent was removed under a stream of N_2, and the resulting residue was washed with MeCN (2 × 0.5 mL) and dried under a stream of N_2 to yield (±)-pseudocopsinine hydrochloride as a white solid. ^{1}H NMR (600 MHz, CD_3OD) δ 7.25−7.20 (m, 1H), 7.07 (td, J = 7.7, 1.2 Hz, 1H), 6.78 (td, J = 7.5, 1.0 Hz, 1H), 6.69 (dt, J = 7.8, 0.8 Hz, 1H), 4.59 (s, 1H), 3.96 (s, 1H), 3.91−3.83 (m, 2H), 3.74 (s, 3H), 3.70 (dt, J = 13.2, 4.7 Hz, 1H), 3.48 (ddd, J = 13.2, 10.4, 4.5 Hz, 1H), 3.36−3.32 (m, 1H), 2.75 (ddd, J = 15.3, 5.8, 2.4 Hz, 1H), 2.48−2.40 (m, 1H), 2.10 (ddd, J = 15.5, 12.3, 1.4 Hz, 1H), 2.06−1.90 (m, 4H), 1.83 (ddd, J = 12.6, 7.6, 4.5 Hz, 1H), 1.66 (dt, J = 13.5, 7.9 Hz, 1H), 1.00 (d, J = 6.8 Hz, 3H); ^{13}C{^{1}H} NMR (151 MHz, CD_3OD) δ 175.5, 150.9, 135.0, 129.7, 124.5, 120.9, 111.9, 81.7, 74.6, 60.8, 57.7, 52.7, 52.1, 44.1, 41.3, 35.8, 34.2, 30.7, 25.8, 20.3, 6.8. The structure and the relative configuration of (±)-pseudocopsinine hydrochloride were unambiguously established with a single crystal X-ray structure determination conducted on a light yellow prism obtained from vapor diffusion between MeOH and Et_2O at −20 °C (CCDC 2015375), see Scheme 6.[35]

(−)-20-epi-Pseudocopsinine ((−)-20-epi-1). Pd/C (10% Pd w/w, 4.5 mg, 0.0042 mmol) was suspended in a solution of (−)-**21** (4.0 mg, 0.0085 mmol) in MeOH (2 mL). The suspension was sparged with H_2 gas for 20 min while being vigorously stirred at 25 °C, then stirred for 16 h at the same temperature under a H_2 atmosphere. The reaction mixture was filtered through Celite, and the filtrate was concentrated under reduced pressure. The residue was purified by PTLC (SiO_2, 5% MeOH/CH_2Cl_2) to afford (−)-**20**-epi-pseudocopsinine (1.7 mg, 58%). ^{1}H NMR (600 MHz, $CDCl_3$) δ 7.27 (m, 1H), 7.06 (td, J = 7.6, 1.1 Hz, 1H), 6.86 (t, J = 7.4 Hz, 1H), 6.78 (d, J = 7.8 Hz, 1H), 3.71 (s, 3H), 3.65 (d, J = 8.5 Hz, 1H), 3.31 (dd, J = 22.0, 16.2 Hz, 3H), 3.09−3.00 (m, 2H), 2.90 (dd, J = 14.1, 6.2 Hz, 1H), 2.17 (dt, J = 14.4, 4.6 Hz, 1H), 1.90 (q, J = 7.3 Hz, 1H), 1.86−1.78 (m, 2H), 1.75 (t, J = 13.1 Hz, 1H), 1.68−1.62 (m, 2H), 1.57 (q, J = 7.3 Hz, 1H), 0.53 (d, J = 7.2 Hz, 3H); ^{13}C{^{1}H} NMR (151 MHz, $CDCl_3$) δ 174.0, 149.8, 127.7, 122.8, 121.9, 112.6, 105.6, 80.0, 73.6, 59.3, 59.1, 54.7, 52.2, 47.8, 43.54, 43.46, 38.0, 35.8, 27.7, 20.3, 9.5; IR (film) ν_{max} 3355, 2930, 1723, 1606, 1482, 1465, 1350, 1322, 1220, 1203, 1152, 1110, 1063, 1018, 924, 828, 747, 699, 653, 621 cm^{-1}; HRMS (ESI-TOF) m/z 339.2064 [(M + H)$^+$, $C_{21}H_{27}N_2O_2^+$, required 339.2073]; $[\alpha]_D^{25}$ −7.5 ± 0.2 (c 0.33, MeOH).

(−)-24. A stirred solution of (−)-**2** (20.0 mg, 0.0425 mmol) and complex 1 (17.4 mg, 0.0425 mmol) in EtOH (10 mL) was sparged with O_2 for 15 min at 25 °C before being treated with 30 μL of $PhSiH_3$ at 3 h intervals until completion (180 μL $PhSiH_3$ added in total, 1.5 mmol). The resulting solution was quenched with the addition of saturated aqueous $Na_2S_2O_4$ (10 mL) and extracted with EtOAc (3 × 5 mL). The combined organic layers were dried over $MgSO_4$ and then concentrated under reduced pressure. The resulting dark brown liquid was loaded onto a silica gel plug which was flushed with hexanes to remove $PhSiH_3$ byproducts, then eluted with 40% EtOAc/hexanes to provide the hydration products as mixture of two diastereomers. The fractions containing the hydration (oxidation) products were concentrated under reduced pressure, and the resulting white foam was purified by PTLC (SiO_2, 60% Et_2O/hexane, developed 3 times) to afford desired diastereomer (−)-**24** (8.3 mg, 38%, R_f: 0.45) and undesired diastereomer (−)-**23** (9.2 mg, 44%, R_f: 0.5) as white powders. For (−)-**23**: ^{1}H NMR (600 MHz, $CDCl_3$) δ 7.76 (dt, J = 7.9, 0.8 Hz, 1H), 7.38−7.28 (m, 5H), 7.23 (qd, J = 7.5, 1.3 Hz, 2H), 7.05 (td, J = 7.5, 1.1 Hz, 1H), 5.35 (d, J = 12.3 Hz, 1H), 5.14 (d, J = 12.4 Hz, 1H), 3.53 (s, 3H), 3.50−3.44 (m, 1H), 3.17 (d, J = 15.8 Hz, 1H), 3.12−3.05 (m, 1H), 2.96−2.90 (m, 2H), 2.37 (ddd, J = 11.5, 8.6, 5.8 Hz, 1H), 2.27 (ddd, J = 12.0, 10.7, 2.9 Hz, 1H), 2.19 (td, J = 11.7, 7.2 Hz, 1H), 2.01 (dd, J = 15.7, 1.9 Hz, 1H), 1.85 (dtt, J = 17.3, 8.6, 4.6 Hz, 1H), 1.76−1.69 (m, 1H), 1.69−1.62 (m, 2H), 1.49 (ddd, J = 13.2, 5.3, 1.8 Hz, 1H), 0.86 (d, J = 6.4 Hz, 3H); ^{13}C{^{1}H} NMR (151 MHz, $CDCl_3$) δ 167.5, 152.5, 150.9, 140.5, 137.9, 135.9, 128.7, 128.4, 128.2, 127.8, 124.2, 120.5, 115.9, 111.4, 68.0, 66.6, 65.8, 53.3, 52.0, 51.8, 51.6, 42.5, 42.2, 28.2, 24.7, 21.9, 17.4; IR (film) ν_{max} 2934, 2781, 1721, 1473, 1460, 1392, 1357, 1327, 1305, 1282, 1250, 1234, 1204, 1181, 1111, 1083, 1048, 752, 698, 616 cm^{-1}; HRMS (ESI-TOF) m/z 489.2391 [(M + H)$^+$, $C_{29}H_{33}N_2O_5^+$, required 489.2389]; $[\alpha]_D^{22}$ −103 (c 0.92, $CHCl_3$). For (−)-**24**: ^{1}H NMR (600 MHz, $CDCl_3$) δ 7.74 (dt, J = 8.1, 0.7 Hz, 1H), 7.40−7.29 (m, 5H), 7.20 (td, J = 7.8, 1.3 Hz, 1H), 7.13 (dd, J = 7.3, 1.3 Hz, 1H), 7.03 (td, J = 7.5, 1.0 Hz, 1H), 5.37 (d, J = 12.3 Hz, 1H), 5.14 (d, J = 12.4 Hz, 1H), 3.55 (s, 3H), 3.50 (q, J = 6.4 Hz, 1H), 3.14−3.10 (m, 1H), 3.09 (d, J = 15.2 Hz, 1H), 2.92 (dd, J = 8.6, 7.1 Hz, 1H), 2.45 (d, J = 1.8 Hz, 1H), 2.40 (dd, J = 15.2, 1.9 Hz, 1H), 2.38−2.33 (m, 1H), 2.25 (td, J = 11.3, 3.1 Hz, 1H), 2.21−2.13 (m, 1H), 1.91−1.79 (m, 1H), 1.68−1.60 (m, 3H), 1.52−1.44 (m, 1H), 0.93 (d, J = 6.4 Hz, 3H); ^{13}C{^{1}H} NMR (151 MHz, $CDCl_3$) δ 168.0, 152.5, 149.6, 140.5, 137.4, 135.9, 128.7, 128.3, 128.3, 127.7, 124.0, 120.6, 115.9, 112.4, 68.0, 67.0, 67.0, 53.4, 52.0, 51.9, 51.7, 42.8, 42.7, 27.5, 25.7, 21.8, 17.6; IR (film) ν_{max} 1940, 2780, 1721, 1473, 1460, 1392, 1356, 1304, 1283, 1253, 1233, 1204, 1181, 1110, 1070, 1049, 754, 732, 636 cm^{-1}; HRMS (ESI-TOF) m/z 489.2387 [(M + H)$^+$, $C_{29}H_{33}N_2O_5^+$, required 489.2389]; $[\alpha]_D^{22}$ −105 (c 0.83, $CHCl_3$).

For **25**: ^{1}H NMR (600 MHz, $CDCl_3$) δ 7.69 (d, J = 8.1 Hz, 1H), 7.51 (dd, J = 7.6, 1.3 Hz, 1H), 7.44−7.30 (m, 5H), 7.22 (td, J = 7.9, 1.4 Hz, 1H), 7.10−7.06 (m, 1H), 5.37 (d, J = 12.3 Hz, 1H), 5.18 (d, J = 12.3 Hz, 1H), 4.08 (q, J = 6.4 Hz, 1H), 3.56 (s, 3H), 3.41 (td, J = 8.8, 5.9 Hz, 1H), 3.29 (dt, J = 12.9, 6.6 Hz, 1H), 3.00 (td, J = 8.6, 2.7 Hz, 1H), 2.90 (dt, J = 11.5, 5.3 Hz, 1H), 2.70 (d, J = 16.3 Hz, 1H), 2.35−2.27 (m, 2H), 2.03−1.96 (m, 1H), 1.82 (ddd, J = 12.1, 6.0, 2.6 Hz, 1H), 1.78−1.71 (m, 2H), 1.41 (dt, J = 13.7, 5.4 Hz, 1H), 1.01 (d, J = 6.4 Hz, 3H); ^{13}C{^{1}H} NMR (151 MHz, $CDCl_3$) δ 167.8, 152.5, 148.6, 140.2, 135.6, 134.3, 128.8, 128.6, 128.5, 127.9, 125.2, 124.4, 115.5, 109.6, 104.6, 81.2, 68.4, 59.4, 51.7, 49.4, 49.1, 43.7, 39.0, 30.3, 27.4, 18.3, 11.6; IR (film) ν_{max} 2945, 1727, 1601, 1462, 1385, 1385, 1350, 1283, 1223, 1134, 1114, 1043, 758, 699 cm^{-1}; HRMS (ESI-TOF) m/z 503.2184 [(M + H)$^+$, $C_{29}H_{31}N_2O_6^+$, required 503.2182].

https://dx.doi.org/10.1021/acs.joc.0c02493
J. Org. Chem. XXXX, XXX, XXX−XXX

(−)-Minovincinine (3). PtO_2 (6.8 mg, 0.025 mmol) was suspended in a solution of (−)-**24** (4.0 mg, 0.0082 mmol) in MeOH (2 mL). The suspension was vigorously stirred and sparged with H_2 for 20 min at 25 °C and then was stirred for 16 h at 25 °C under a H_2 atmosphere. The reaction mixture was filtered through Celite, and the filtrate was concentrated under reduced pressure. The crude residue was purified by PTLC (SiO_2, 60% EtOAc/hexane) to afford (−)-minovincinine (**3**, 2.9 mg, 99%). Synthetic (−)-minovincinine is spectroscopically identical to that reported for naturally isolated material as reported by Williams et al.[17] ^{1}H NMR (600 MHz, acetone-d_6) δ 9.16 (s, 1H), 7.26 (d, J = 7.4 Hz, 1H), 7.10 (td, J = 7.7, 1.2 Hz, 1H), 7.00 (dt, J = 7.8, 0.8 Hz, 1H), 6.83 (td, J = 7.4, 1.0 Hz, 1H), 3.66 (s, 3H), 3.42−3.35 (m, 1H), 3.14−3.07 (m, 1H), 2.98 (d, J = 5.3 Hz, 1H), 2.89 (dd, J = 8.3, 6.5 Hz, 1H), 2.75 (d, J = 14.6 Hz, 1H), 2.68 (dd, J = 14.7, 1.9 Hz, 1H), 2.65 (d, J = 1.8 Hz, 1H), 2.54 (ddd, J = 11.6, 8.3, 4.7 Hz, 1H), 2.40 (td, J = 10.6, 3.6 Hz, 1H), 1.99 (td, J = 11.5, 6.5 Hz, 1H), 1.87−1.77 (m, 1H), 1.61 (m, 3H), 1.52 (ddd, J = 13.4, 12.0, 4.7 Hz, 1H), 0.86 (d, J = 6.5 Hz, 3H); ^{13}C{^{1}H} NMR (151 MHz, acetone-d_6) δ 169.3, 168.0, 144.9, 138.1, 128.3, 121.6, 121.1, 110.5, 93.2, 68.8, 67.0, 56.2, 52.2, 51.4, 50.9, 46.6, 43.8, 26.9, 26.5, 22.7, 18.3; IR (film) ν_{max} 3365, 2933, 1776, 1668, 1605, 1463, 1438, 1371, 1296, 1279, 1253, 1235, 1154, 1129, 1104, 1044, 902, 796, 745 cm^{-1}; HRMS (ESI-TOF) m/z 355.2023 [(M + H)$^+$, $C_{21}H_{27}N_2O_3^+$, required 355.2022]; $[\alpha]_D^{25}$ −497 ± 1 (c 0.07, MeOH), Janot and coworkers[15] reported $[\alpha]_D^{20}$ −504 ± 5 (c 0.5, EtOH), De Luca and coworkers[17] reported $[\alpha]_D^{20}$ −514 (c 0.07, MeOH).

(−)-20-epi-Minovincinine ((−)-20-epi-3). PtO_2 (6.8 mg, 0.025 mmol) was suspended in a solution of (−)-**23** (4.0 mg, 0.0082 mmol) in MeOH (2 mL). The suspension was vigorously stirred and sparged with H_2 for 20 min at 25 °C, then was stirred for 16 h at 25 °C under a H_2 atmosphere. The reaction mixture was filtered through Celite and the filtrate was concentrated under reduced pressure. The crude residue was purified by PTLC (SiO_2, 60% EtOAc/hexane) to afford (−)-**20**-epi-minovincinine (2.6 mg, 89%). ^{1}H NMR (600 MHz, acetone-d_6) δ 9.20 (s, 1H), 7.25 (d, J = 7.3 Hz, 1H), 7.10 (td, J = 7.6, 1.2 Hz, 1H), 7.03−6.95 (m, 1H), 6.86−6.79 (m, 1H), 3.69 (s, 3H), 3.26 (p, J = 6.2 Hz, 1H), 3.21 (s, 1H), 3.09 (m, 2H), 2.94−2.85 (m, 2H), 2.60 (s, 1H), 2.44 (t, J = 10.3 Hz, 1H), 2.26 (d, J = 15.2 Hz, 1H), 2.01−1.85 (m, 2H), 1.80 (d, J = 13.4 Hz, 1H), 1.62 (m, 2H), 1.42 (d, J = 13.4 Hz, 1H), 0.84 (d, J = 6.4 Hz, 3H); ^{13}C{^{1}H} NMR (151 MHz, acetone-d_6) δ 168.6, 168.3, 144.4, 138.8, 128.1, 122.1, 121.1, 110.3, 91.8, 67.6, 67.1, 56.4, 52.1, 50.9, 50.8, 46.6, 43.2, 27.3, 25.5, 22.7, 17.8; IR (film) ν_{max} 3373, 2936, 2777, 1671, 1605, 1463, 1437, 1377, 1296, 1278, 1253, 1237, 1201, 1154, 1130, 1105, 1045, 897, 795, 746, 659 cm^{-1}; HRMS (ESI-TOF) m/z 355.2026 [(M + H)$^+$, $C_{21}H_{27}N_2O_3^+$, required 355.2022]; $[\alpha]_D^{25}$ −429 (c 0.07, MeOH).

■ ASSOCIATED CONTENT

Supporting Information

The Supporting Information is available free of charge at https://pubs.acs.org/doi/10.1021/acs.joc.0c02493.

Experimental details for Scheme 3, representative optimization of cyclization of **2**, tabulation of ^{1}H and ^{13}C NMR data for synthetic **1**, 20-epi-**1**, and reported data, representative optimization of olefin oxidation of **2**, X-ray details for **1**, and copies of ^{1}H and ^{13}C{^{1}H} NMR spectra (PDF)

Accession Codes

CCDC 2015375 contains the supplementary crystallographic data for this paper. These data can be obtained free of charge via www.ccdc.cam.ac.uk/data_request/cif, or by emailing data_request@ccdc.cam.ac.uk, or by contacting The Cambridge Crystallographic Data Centre, 12 Union Road, Cambridge CB2 1EZ, UK; fax: +44 1223 336033.

■ AUTHOR INFORMATION

Corresponding Author

Dale L. Boger − *Department of Chemistry and the Skaggs Institute for Chemical Biology, The Scripps Research Institute, La Jolla, California 92037, United States;* orcid.org/0000-0002-3966-3317; Email: boger@scripps.edu

Authors

Xianhuang Zeng − *Department of Chemistry and the Skaggs Institute for Chemical Biology, The Scripps Research Institute, La Jolla, California 92037, United States*

Vyom Shukla − *Department of Chemistry and the Skaggs Institute for Chemical Biology, The Scripps Research Institute, La Jolla, California 92037, United States*

Complete contact information is available at: https://pubs.acs.org/10.1021/acs.joc.0c02493

Notes

The authors declare no competing financial interest.

■ ACKNOWLEDGMENTS

We are especially grateful for the financial support of NIH (CA042056, D.L.B.). We thank Milan Gembicky of the X-ray Crystallography Facility at University of California, San Diego for X-ray structure determination of (±)-**1**; Britanny Sanchez, Emily Sturgell, and Jason Chen of Automated Synthesis Facility at TSRI for chiral chromatographic separation of **12** and HRMS of compounds; and Dee-Hua Huang and Laura Pasternack for NMR assistance.

■ REFERENCES

(1) Abdurakhimova, N.; Yuldashev, P. K.; Yunusov, S. Y. The structure of majdine, pseudokopsinine, and vinervinine. *Chem. Nat. Compd.* **1967**, *3*, 263−266.

(2) (a) Nasyrov, S.-M.; Andrianov, V. G.; Struchkov, Y. T. X-Ray structure and absolute configuration of (−)-pseudocopsinine. *J. Chem. Soc., Chem. Commun.* **1974**, 979. (b) Adizov, S. M.; Tashkhodzhaev, B.; Kunafiev, R. Z.; Mirzaeva, M. M.; Yuldashev, P. K. *J. Struct. Chem.* **2017**, *58*, 291.

(3) Parsons, P. J.; Penkett, C. S.; Cramp, M. C.; West, R. I.; Warrington, J.; Saraiva, M. C. Tandem radical cyclisation reactions for the construction of pseudocopsinine and aspidosperma alkaloid models. *Synlett* **1995**, 507−509.

(4) Parsons, P. J.; Penkett, C. S.; Cramp, M. C.; West, R. I.; Warren, E. S. The facile construction of indole alkaloid models: A tandem cascade approach for the synthesis of a model for pseudocopsinine. *Tetrahedron* **1996**, *52*, 647−660.

(5) Hugel, G.; Cossy, J.; Levy, J. A biomimetic entry in the hexacyclic tuboxenin ring system methylene-indolines, indolenines and indoleniniums, XXII. *Tetrahedron Lett.* **1987**, *28*, 1773−1775.

(6) Hugel, G.; Cartier, D.; Lévy, J. Synthesis of hexacyclic indole alkaloids related to vindolinine by sonochemical cyclization. *Tetrahedron Lett.* **1989**, *30*, 4513−4516.

(7) (a) Ishikawa, H.; Colby, D. A.; Seto, S.; Va, P.; Tam, A.; Kakei, H.; Rayl, T. J.; Hwang, I.; Boger, D. L. Total synthesis of vinblastine, vincristine, related natural products and key structural analogues. *J. Am. Chem. Soc.* **2009**, *131*, 4904−4916. (b) Ishikawa, H.; Colby, D. A.; Boger, D. L. Direct coupling of catharanthine and vindoline to provide vinblastine: total synthesis of (+)- and *ent*-(−)-vinblastine. *J. Am. Chem. Soc.* **2008**, *130*, 420−421. (c) Leggans, E. K.; Barker, T. J.; Duncan, K. K.; Boger, D. L. Iron(III)/$NaBH_4$-mediated additions to unactivated alkenes: Synthesis of novel 20′-vinblastine analogues. *Org. Lett.* **2012**, *14*, 1428−1431. (d) Barker, T. J.; Boger, D. L. Fe(III)/$NaBH_4$-mediated free radical hydrofluorination of unactivated alkenes. *J. Am. Chem. Soc.* **2012**, *134*, 13588−13591.

(8) (a) Lo, J. C.; Kim, D.; Pan, C.-M.; Edwards, J. T.; Yabe, Y.; Gui, J.; Qin, T.; Gutierrez, S.; Giacoboni, J.; Smith, M. W.; Holland, P. L.; Baran, P. S. Fe-Catalyzed C-C bond construction from olefins via radicals. *J. Am. Chem. Soc.* **2017**, *139*, 2484−2503. (b) Crossley, S. W. M.; Barabe, F.; Shenvi, R. A. Simple, chemoselective, catalytic olefin isomerization. *J. Am. Chem. Soc.* **2014**, *136*, 16788−16791.

(9) Corey, E. J.; Howe, W. J.; Orf, H. W.; Pensak, D. A.; Petersson, G. General methods of synthetic analysis. Strategic bond disconnections for bridged polycyclic structures. *J. Am. Chem. Soc.* **1975**, *97*, 6116−6124.

(10) (a) Liu, J.; Ma, D. A Unified approach for the assembly of atisine- and hetidine-type diterpenoid alkaloids: Total syntheses of azitine and the proposed structure of navirine C. *Angew. Chem., Int. Ed.* **2018**, *57*, 6676−6680. (b) Kerschgens, I.; Rovira, A. R.; Sarpong, R. Total synthesis of (−)-xishacorene B from (R)-carvone using a C-C activation strategy. *J. Am. Chem. Soc.* **2018**, *140*, 9810−9813.

(11) (a) George, D. T.; Kuenstner, E. J.; Pronin, S. V. A concise approach to paxilline indole diterpenes. *J. Am. Chem. Soc.* **2015**, *137*, 15410−15413. (b) Deng, H.; Cao, W.; Liu, R.; Zhang, Y.; Liu, B. Asymmetric total synthesis of hispidanin A. *Angew. Chem., Int. Ed.* **2017**, *56*, 5849−5852. (c) Lu, Z.; Zhang, X.; Guo, Z.; Chen, Y.; Mu, T.; Li, A. Total synthesis of aplysiasecosterol A. *J. Am. Chem. Soc.* **2018**, *140*, 9211−9218. (d) Xu, G.; Wu, J.; Li, L.; Lu, Y.; Li, C. Total synthesis of (−)-daphnezomines A and B. *J. Am. Chem. Soc.* **2020**, *142*, 15240−15245. (e) Li, J.; Li, F.; King-Smith, E.; Renata, H. Merging chemoenzymatic and radical-based retrosynthetic logic for rapid and modular synthesis of oxidized meroterpenoids. *Nat. Chem.* **2020**, *12*, 173−179. (f) Bartels, F.; Weber, M.; Christmann, M. Synthesis of spongidine A and D and petrosaspongiolide L methyl ester using pyridine C-H functionalization. *Org. Lett.* **2020**, *22*, 552−555. (g) Ruider, S. A.; Sandmeier, T.; Carreira, E. M. Total synthesis of (±)-hippolachnin A. *Angew. Chem., Int. Ed.* **2015**, *54*, 2378−2382.

(12) (a) Elliott, G. I.; Fuchs, J. R.; Blagg, B. S. J.; Ishikawa, H.; Tao, H.; Yuan, Z. Q.; Boger, D. L. Intramolecular Diels-Alder/1,3-dipolar cycloaddition cascade of 1,3,4-oxadiazoles. *J. Am. Chem. Soc.* **2006**, *128*, 10589−10595. (b) Wilkie, G. D.; Elliott, G. I.; Blagg, B. S. J.; Wolkenberg, S. E.; Soenen, D. R.; Miller, M. M.; Pollack, S.; Boger, D. L. Intramolecular Diels-Alder and tandem intramolecular Diels-Alder/1,3-dipolar cycloaddition reactions of 1,3,4-oxadiazoles. *J. Am. Chem. Soc.* **2002**, *124*, 11292−11294.

(13) (a) Sears, J. E.; Boger, D. L. Tandem intramolecular Diels-Alder/1,3-dipolar cycloaddition cascade of 1,3,4-oxadiazoles: initial scope and applications. *Acc. Chem. Res.* **2016**, *49*, 241−251. (b) Zhang, J.; Shukla, V.; Boger, D. L. Inverse electron demand Diels-Alder reactions of heterocyclic azadienes, 1-aza-1,3-butadienes, cyclopropenone ketals, and related systems. A retrospective. *J. Org. Chem.* **2019**, *84*, 9397−9445.

(14) Crossley, S. W. M.; Obradors, C.; Martinez, R. M.; Shenvi, R. A. Mn-, Fe-, and Co-Catalyzed radical hydrofunctionalizations of olefins. *Chem. Rev.* **2016**, *116*, 8912−9000.

(15) Plat, M.; Men, J. L.; Janot, M.-M. Structure de quatre alcaloides de la Petite Pervenche (*Vinca minor* L.): (−)-vincadifformine, minovincine, minovincine et methoxy-16-minovincine. Alcaloides des pervenches. Application de la spectrographie de masse aux problemes de determinatino de structure et de stereochimie (partie XVII). *Bull. Soc. Chim. Fr.* **1962**, 2237−2241.

(16) Majumder, P. L.; Basu, A. Absolute configuration at C-19 of 19-hydroxy/acyloxy-(+)-vincadifformine type of alkaloids. *Indian J. Chem.* **1985**, *24B*, 649−650.

(17) Williams, D.; Qu, Y.; Simionescu, R.; De Luca, V. The assembly of (+)-vincadifformine- and (−)-tabersonine-derived monoterpenoid indole alkaloids in Catharanthus roseus involves separate branch pathways. *Plant J.* **2019**, *99*, 626−636.

(18) Sun, J.; Zhao, L.; Shao, Z.; Shanks, J.; Peebles, C. A. M. Expression of tabersoninine 16-hydroxylase and 16-hydroxytabersonine-O-methyltransferase in Catharanthus roseus hairy roots. *Biotechnol. Bioeng.* **2018**, *115*, 679−683.

(19) Carqueijeiro, I.; Dugéde Bernonville, T.; Lanoue, A.; Dang, T.-T.; Teijaro, C. N.; Paetz, C.; Billet, K.; Mosquera, A.; Oudin, A.; Besseau, S.; Papon, N.; Glévarec, G.; Atehortùa, L.; Clastre, M.; Giglioli-Guivarc'h, N.; Schneider, B.; St-Pierre, B.; Andrade, R. B.; O'Connor, S. E.; Courdavault, V. A BAHD acyltransferase catalyzing 19-O-acetylation of tabersonine derivatives in roots of Catharanthus roseus enables combinatorial synthesis of monoterpene indole alkaloids. *Plant J.* **2018**, *94*, 469−484.

(20) Abouzeid, S.; Beutling, U.; Selmar, D. Stress-induced modification of indole alkaloids: Phytomodificines as a new category of specialized metabolites. *Phytochemistry* **2019**, *159*, 102−107.

(21) Langlois, N.; Andriamialisoa, R. Z. Studies on vindolinine. 6. Partial synthesis of aspidospermane-type alkaloids. *J. Org. Chem.* **1979**, *44*, 2468−2471.

(22) Lee, K.; Boger, D. L. Total synthesis of (−)-kopsinine and ent-(+)-kopsinine. *Tetrahedron* **2015**, *71*, 3741−3746.

(23) Xie, J.; Wolfe, A. L.; Boger, D. L. Total synthesis of kopsinine. *Org. Lett.* **2013**, *15*, 868−870.

(24) (a) Campbell, E. L.; Zuhl, A. M.; Liu, C. M.; Boger, D. L. Total synthesis of (+)-fendleridine (aspidoalbidine) and (+)-1-acetylaspidoalbidine. *J. Am. Chem. Soc.* **2010**, *132*, 3009−3012. (b) Cycloaddition of **9** to provide **8** was run in two batches as described. The first batch (10 g **9**, 16.2 mmol) yielded **8** (7.6 g, 13.6 mmol, 84%) in seven runs conducted at ca. 1.5 g scales before being combined and purified. The second batch (11.2 g **9**, 18.2 mmol) yielded **8** (7.5 g, 13.4 mmol, 74%) over eight runs at ca. 1.5 g scales.

(25) Lee, K.; Boger, D. L. Total syntheses of (−)-kopsifoline D and (−)-deoxoapodine: Divergent total synthesis via late-stage key strategic bond formation. *J. Am. Chem. Soc.* **2014**, *136*, 3312−3317.

(26) Boger, D. L.; Brotherton, C. E. Total synthesis of azafluoranthene alkaloids: rufescine and imeluteine. *J. Org. Chem.* **1984**, *49*, 4050−4055.

(27) Sharpless, K. B.; Lauer, R. F. Mild procedure for the conversion of epoxides to allylic alcohols. First organoselenium reagent. *J. Am. Chem. Soc.* **1973**, *95*, 2697−2699.

(28) Hayashi, Y.; Inagaki, F.; Mukai, C. Total synthesis of (±)-meloscine. *Org. Lett.* **2011**, *13*, 1778−1780.

(29) Kang, E. J.; Cho, E. J.; Ji, M. K.; Lee, Y. E.; Shin, D. M.; Choi, S. Y.; Chung, Y. K.; Kim, J.-S.; Kim, H.-J.; Lee, S.-G.; Lah, M. S.; Lee, E. Stereoselective synthesis of (+)-SCH 351448: A unique ligand system for sodium, calcium, and other cations. *J. Org. Chem.* **2005**, *70*, 6321−6329.

(30) Detty, M. R. Oxidation of selenides and tellurides with positive halogenating species. *J. Org. Chem.* **1980**, *45*, 274−279.

(31) Obradors, C.; Martinez, R. M.; Shenvi, R. A. Ph(i-PrO)SiH_2: An exceptional reductant for metal-catalyzed hydrogen atom transfers. *J. Am. Chem. Soc.* **2016**, *138*, 4962−4971.

(32) Kim, D.; Rahaman, S. M. W.; Mercado, B. Q.; Poli, R.; Holland, P. L. Roles of iron complexes in catalytic radical alkene cross-coupling: A computational and mechanistic study. *J. Am. Chem. Soc.* **2019**, *141*, 7473−7485.

(33) Yagudaev, M. R. The NMR study of alkaloids. VI. A comparison of the stereochemistries of pseudocopsinine and 14,15-dihydrovindolinine by ^{13}C NMR spectroscopy. *Chem. Nat. Compd.* **1984**, *20*, 311−314.

(34) Ahond, A.; Janot, M. M.; Langlois, N.; Lukacs, G.; Potier, P.; Rasoanaivo, P.; Sangare, M.; Neuss, N.; Plat, M.; LeMen, J.; Hagaman, E. W.; Wenkert, E. Carbon-13 nuclear magnetic resonance spectroscopy of naturally occurring substances. XXIII. Structure of vindolinine. *J. Am. Chem. Soc.* **1974**, *96*, 633−634.

(35) The structure and relative stereochemistry of **1** as its hydrochloride salt were unambiguously established in a single-crystal X-ray structure determination conducted on a light yellow prism obtained by vapor diffusion between MeOH and Et_2O at −20 °C and has been deposited with the Cambridge Crystallographic Data Center (CCDC 2015375).

(36) Ruider, S. A.; Sandmeier, T.; Carreira, E. M. Total synthesis of (±)-hippolachnin A. *Angew. Chem., Int. Ed.* **2015**, *54*, 2378−2382.

(37) Lin, B.; Shi, S.; Lin, R.; Cui, Y.; Fang, M.; Tang, G.; Zhao, Y. Cobalt-catalyzed oxidative C(sp^3)-H phosphonylation for α-amino-

https://dx.doi.org/10.1021/acs.joc.0c02493
J. Org. Chem. XXXX, XXX, XXX−XXX

phosphonates via C(sp^3)-H/P(O)-H coupling. *J. Org. Chem.* **2018**, *83*, 6754−6761.
(38) Ratnikov, M. O.; Doyle, M. P. Mechanistic investigation of oxidative Mannich reaction with tert-butyl hydroperoxide. The role of transition metal salt. *J. Am. Chem. Soc.* **2013**, *135*, 1549−1557.
(39) (a) Hamilton, D. E.; Drago, R. S.; Telser, J. Spin trapping of a cobalt-dioxygen complex. *J. Am. Chem. Soc.* **1984**, *106*, 5353−5355. (b) Tokuyasu, T.; Kunikawa, S.; Masuyama, A.; Nojima, M. Co(III)-Alkyl complex- and Co(III)-alkylperoxo complex-catalyzed triethylsilylperoxidation of alkenes with molecular oxygen and triethylsilane. *Org. Lett.* **2002**, *4*, 3595−3598.
(40) Mukaiyama, T.; Yamada, T. Recent advances in aerobic oxygenation. *Bull. Chem. Soc. Jpn.* **1995**, *68*, 17−35.
(41) An alternative involves first alkene functionalization to the corresponding secondary hydroperoxy radical followed by a subsequent C19 oxidation perhaps by 1,5-HAT and peroxide ring closure but requires invoking a initial diastereoselective C20 oxidation.

https://dx.doi.org/10.1021/acs.joc.0c02493
J. Org. Chem. XXXX, XXX, XXX−XXX